Optics Communications ■ (■■■■) ■■■–■■■

Contents lists available at ScienceDirect

Optics Communications

journal homepage: www.elsevier.com/locate/optcom

Invited Paper

Dynamic localization of light in squeezed-like photonic lattices

M. Khazaei Nezhad [a,c,*], M. Golshani [b,c], S.M. Mahdavi [c,d], A.R. Bahrampour [c], A. Langari [c,e]

[a] Department of Physics, Faculty of Sciences, Ferdowsi University of Mashhad, Mashhad, Iran
[b] Faculty of Physics, Shahid Bahonar University of Kerman, Kerman, Iran
[c] Department of Physics, Sharif University of Technology, P.O. Box: 11155-9161 Tehran, Iran
[d] Institute for Nanoscience and Nanotechnology, Sharif University of Technology, Tehran 15614, Iran
[e] Center of Excellence in Complex Systems and Condensed Matter (CSCM), Sharif University of Technology, Tehran 1458889694, Iran

ARTICLE INFO

Article history:
Received 27 August 2015
Received in revised form
27 January 2016
Accepted 28 January 2016

Keywords:
Dynamic localization
Squeezed photonic lattices
Waveguide arrays

ABSTRACT

We investigate the dynamic localization of light in the sinusoidal bent squeezed-like photonic lattices, a class of inhomogeneous semi-infinite waveguide arrays. Our findings show that, dynamic localization takes place for the normalized amplitude of sinusoidal profile (α) above a critical value α_c. In this regime, for any normalized amplitude $\alpha > \alpha_c$, there is a specific spatial period (ℓ) of waveguides, in which the dynamical oscillation, with the same spatial period occurs. Moreover, the specific spatial period is a decreasing function of the normalized amplitude α. Accordingly, the dynamical oscillation and self-imaging is realized, in spite of the existence of inhomogeneous coupling coefficients and semi-infinite nature of the squeezed-like photonic lattices. In addition, a comparison between the dynamic localization and Bloch oscillation in squeezed-like photonic lattices reveals that for the same values of α ($>\alpha_c$), the variation in the width and the mean center of the Bloch oscillation profile are less than the corresponding values of the dynamic localization. Also, we propose the experimental conditions to observation of dynamic localization in squeezed photonic lattices.

1. Introduction

Dynamic localization (DL) and Bloch oscillations (BO) are two examples of coherent destruction of quantum tunneling for electron wave packet in a super lattice, in the presence of external forces [1,2].

If a constant force is exerted on an electronic super lattice, the extended Bloch wave functions are converted to the localized Wannier states, and the energy levels of the lattice form the equidistant Wannier–Stark ladders [1,3–5]. In this case, the electrons show the periodic motion known as Bloch oscillation [1]. Similar periodic motion is also observed for light waves propagation in the array of optical waveguides owning a transverse linear gradient in their propagation constants. In such arrays, the propagation direction plays the role of time, and hence the periodic motion is known as the spatial Bloch oscillations [6–9].

Instead of a constant force, if a periodic electric field is applied to an electronic super lattice, under a certain condition, the other type of cancellation of quantum diffusion can be observed [2–5]. In this case, for the special filed amplitudes, frequencies and the lattice constants, the quantum tunneling can be stopped and the electrons oscillate, near their initial positions, with a frequency equal to the frequency of the driven field [2–5]. This type of periodic motion is known as the dynamic localization and is related to the collapse of quasi-energy minibands in the supper lattices [3–5,10]. This conditional periodic motion is also observed, for the light waves, in the 1D and 2D curved photonic lattices, where the sinusoidal bending profile of the guides plays the role of periodic force [11–13].

In the previous works, some different aspects of DL have been investigated [14–17], for instance, the effects of disorder, defects and hopping to all neighbors. However, little is known on DL in semi-infinite and inhomogeneous lattices. In a homogeneous semi-infinite lattice, the application of the sinusoidal force can lead to the dynamically preserved surface states [18,19], which prevent the self collimation of beam when the wave packet reaches the lattice boundary. In Refs. [20,21], the authors introduced Glauber–Fock (GF) photonic lattice, which is a class of semi-infinite inhomogeneous lattices. This lattice can be implemented to simulate classically, some interesting phenomena in quantum optics, such as quantum random walk, and photon bunching and anti-bunching [21–23]. They also investigated the DL in the GF lattice [24], and derived the condition for demonstration of DL, similar to the condition in homogeneous infinite lattices.

* Corresponding author at: Department of Physics, Faculty of Sciences, Ferdowsi University of Mashhad, Mashhad, Iran.
E-mail addresses: khazaii64@gmail.com, khazaeinezhad@um.ac.ir (M.K. Nezhad).

http://dx.doi.org/10.1016/j.optcom.2016.01.082
0030-4018/

In our previous work [25], we introduced another type of semi-infinite photonic lattices incorporating inhomogeneous coupling terms. This lattice provides the classical analogs to the squeezed intensity distribution in quantum optics, and was called squeezed photonic lattice. In that work, we also investigated the phase transition to the spatial BO, by adding the transverse linear gradient in propagation constants of each guides of the lattice.

The aim of this paper is to investigate the conditions for DL in sinusoidal bent squeezed photonic lattice. DL can be observed under a certain condition on the bending profile of the guides, in spite of the fact that the semi-infinite nature and inhomogeneity of coupling coefficients of this lattice are similar to the GF lattice. Moreover, we discuss how the distribution profile of a Gaussian input is affected by DL compared with a single-site excitation. We also address the similar features of DL and BO, while their origins are being different. we discussed the accessible experimental conditions to see DL.

This paper is organized in four sections. Section 2 is devoted to the theoretical model for light propagation in curved squeezed lattices. Numerical results and discussion are presented in Section 3. Finally, we conclude and summarize our results in Section 4.

2. Theoretical model

In our previous work [25], the squeezed photonic lattice, containing two separate linear arrays of optical waveguides with the specific coupling coefficients, were introduced to simulate classically the quantum (number and coherent) squeezed states. Here, we consider one of these decoupled arrays, the lower one, and call it the *squeezed-like photonic lattice*, since some expected phenomena, such as coherent squeezed photon number distribution, cannot be simulated classically with this array.

To investigate DL, an array of sinusoidal bending squeezed-like photonic lattice is considered (see Fig. 1). As shown in Fig. 1, the optical axis of waveguides has sinusoidal bending profile $x(z) = A\cos(\frac{2\pi}{L}z)$ with amplitude A and spatial period L, where $L \gg A$ to ignore the radiation loss due to the bending of guides. The adjacent waveguides are separated by the same distance d along the x-axis, while their distance decrease along the y-axis such that the coupling coefficients have inhomogeneous pattern similar to the squeezed-like photonic lattice (see [24,26]).

The slowly varying envelope approximation (SVEA) is implemented to write the light propagation equation in the considered curved waveguide array. In this approximation, the governing equation of electric field amplitude $E_n(z)$, at the n-th waveguide ($n = 0, 1, 2, \ldots$), is reduced to the following tight-binding (TB) model [3,27,28]:

$$i\frac{dE_n(z)}{dz} + K_nE_n + C_nE_{n-1} + C_{n+1}E_{n+1} - n\omega\ddot{x}_0(z)E_n(z) = 0, \tag{1}$$

where K_n is the propagation constant of the n-th waveguide, and $C_n = C\sqrt{2n(2n-1)}$ is the coupling coefficient between the $(n-1)$-th and the n-th waveguides. Due to the exponential decay of the coupling coefficient with increasing waveguide separation [29], to gain this form of coupling coefficient, one must change the distances between adjacent waveguides along the y-axis as $d_n = d_1 - \frac{\kappa d}{2d_1}\ln(n(2n-1))$. Here d_n and κ are the distance between $n-1$ and n waveguide along y-axis and the *FWHM* of single modal field in each waveguide, respectively [28]. In our study, we consider identical waveguides and assume $K_n = K_0$. Moreover, $\omega = \frac{2\pi n_s d}{\lambda}$ is the normalized frequency, where n_s and λ are the refractive index of substrate and the wavelength of incident light, respectively, and finally $\ddot{x}_0(z)$ shows the curvature of waveguides.

We introduce the new variables $Z = Cz$, $l = CL$, $\alpha = \frac{A\omega}{2C}(\frac{2\pi}{L})^2$ and $E_n(z) = \Psi_n(Z)\exp(i\frac{K_0}{C}Z)$, which transform Eq. (1) to the following dimensionless form:

$$i\frac{d\Psi_n}{dZ}(Z) + \sqrt{2n(2n-1)}\Psi_{n-1}(Z) + \sqrt{(2n+1)(2n+2)}\Psi_{n+1}(Z) + 2n\alpha\cos\left(\frac{2\pi}{l}Z\right)\Psi_n(Z) = 0. \tag{2}$$

In order to find the solution of Eq. (2), the following operator relation is defined:

$$i\frac{d\Phi}{dZ}(Z) = -\left(\hat{a}^2 + \alpha\cos\left(\frac{2\pi}{l}Z\right)\hat{a}^\dagger\hat{a} + \hat{a}^{\dagger 2}\right)\Phi(Z) = -\hat{H}(Z)\Phi(Z), \tag{3}$$

where $\Phi(Z) \equiv \sum_m \Psi_m(Z)|2m\rangle$, and $|2m\rangle$ represents the classical analogue of Fock states, which denotes the optical mode of the m-th waveguide. (It should be noticed that the squeezed-like photonic lattice is the even-labeled chain of squeezed photonic lattice [25]; see Fig. 1.) The set $\{|m\rangle\}$ is called the waveguide number basis and $\Psi_m(Z)$ denotes the amplitude of electric field in the m-th waveguide at dimensionless propagation distance Z. Moreover, $\hat{a}$ and $\hat{a}^\dagger$ are peculiar translation operators to the left and right, respectively, which are defined by $\hat{a}|m\rangle = \sqrt{m}|m-1\rangle$ and $\hat{a}^\dagger|m\rangle = \sqrt{m+1}|m+1\rangle$ that are similar to the bosonic annihilation and creation operators of quantum optics [25].

Applying usual orthogonality of the eigenmodes of each guides which causes the orthogonality of waveguide number basis ($\langle m|n\rangle = \delta_{m,n}$), it is straightforward to show that Eq. (3) is the operator form of Eq. (2). Hence, we solve Eq. (3) instead of Eq. (2).

The dynamical equation appeared in Eq. (3) is a Z-dependent Hamiltonian similar to the time dependent Hamiltonian in quantum mechanics. The solution of this equation can be written as Dyson series [30]:

$$\Phi(Z) = \overleftrightarrow{T}\left[\exp\left\{i\int_0^Z \hat{H}(Z')\,dZ'\right\}\right]\Phi(Z=0), \tag{4}$$

where $\overleftrightarrow{T}$ denotes the Z-ordered operator. There is no general solution for Z-depended Hamiltonian, while for special cases of Z-depended operators, a solution can be found.

Applying the Lie algebra and the disentangling theorem, we can rewrite Eq. (4) as follows [30]:

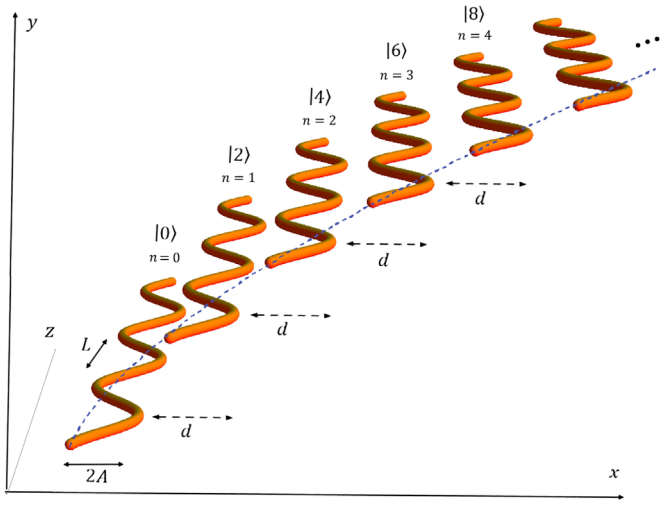

Fig. 1. Sinusoidal squeezed-like photonic lattice.

$$\Phi(Z) = \exp\left[-\frac{i\alpha l}{4\pi}\sin\left(\frac{2\pi}{l}Z\right)\right]\exp[\phi_+(Z)\,\widehat{K}_+]$$

$$\times \exp[\phi_z(Z)\widehat{K}_z]\exp[\phi_-(Z)\,\widehat{K}_-]\Phi(Z=0) = \hat{S}_{(\alpha,l)}(Z)\Phi(Z=0), \tag{5}$$

Here, $\widehat{K}_+ = \frac{\hat{a}^{\dagger 2}}{2}$, $\widehat{K}_- = \frac{\hat{a}^2}{2}$ and $\widehat{K}_z = \frac{1}{2}(\hat{a}^\dagger\hat{a} + \frac{1}{2})$ are the SU(1, 1) Lie generators. $\phi_+(Z)$, $\phi_-(Z)$ and $\phi_z(Z)$ are determined by the following differential equations [30]:

$$\frac{d\phi_+}{dZ}(Z) = 2i\left[\phi_+(Z)^2 + \alpha\cos\left(\frac{2\pi}{l}Z\right)\phi_+(Z) + 1\right], \tag{6}$$

$$\frac{d\phi_z(Z)}{dZ} = 2i\left[2\phi_+(Z) + \alpha\cos\left(\frac{2\pi}{\ell}Z\right)\right], \tag{7}$$

$$\frac{d\phi_-(Z)}{dZ} = 2i\exp\left[\phi_z(Z)\right], \tag{8}$$

with the following initial conditions:

$$\phi_+(0) = \phi_-(0) = \phi_z(0) = 0. \tag{9}$$

Let us consider the array is being excited by an input at the n-th waveguide, the electric filed amplitude in the m-th waveguide, at the propagation distance Z, is given by $\Psi_m^{(n)}(Z) = \left\langle 2m\middle|\hat{S}_{\alpha,\ell}(Z)\middle|2n\right\rangle$, which can be obtained by employing the evolution operator of Eq. (5),

$$\Psi_m^{(n)}(Z) = \sqrt{(2n)!(2m)!}\,\exp\left[-\frac{i\alpha\ell}{4\pi}\sin\left(\frac{2\pi}{\ell}Z\right) + \frac{1}{4}\phi_z\left(Z\right)\right]$$

$$\times \sum_{p=0}^{\min\{m,n\}} \frac{\left[\phi_+(Z)\right]^{m-p}\left[\phi_-(Z)\right]^{n-p}\exp\left[p\phi_z(Z)\right]}{2^{m+n-2p}(n-p)!\left(m-p\right)!(2p)!}. \tag{10}$$

According to Eq. (5), the exponential operators $\exp[\phi_\pm(Z)\,\widehat{K}_\pm]$ are responsible for the coupling of light to the right and left waveguides. If at a special dimensionless propagation distance Z, $\phi_\pm(Z)$ vanish simultaneously, there is no coupling of the light to the left and right waveguides, which is the signature of light localization. The periodic coincidence of $\phi_\pm(Z) = 0$ at each period of bending waveguides manifests the presence of DL, which causes light to return to the initial injected guide periodically. In the other word when the conditions for DL is satisfied, the group velocity dispersion tends to zero after each period of guides. It is straightforward to show that, under conditions in which $\phi_\pm(Z = m\ell) = 0$, then $\phi_z(Z = m\ell) = 0$ and $\Psi_p^{(q)}(Z = m\ell) = \delta_{p,q}$.

3. Numerical results and discussion

The system of equations (2) cannot be solved analytically. This leads us to implement numerical simulation to study the behavior of $\phi_\pm(Z)$ and $\phi_z(Z)$ for different values of normalized amplitude α and normalized spatial period ℓ.

Fig. 2(a) and (b) shows the absolute values of the solution of equations (2), for two different values of (α, ℓ). As shown in these figures, for the values of $(\alpha = 6.5, \ell = 1.2477)$, $\phi_\pm(Z)$ and $\phi_z(Z)$ are periodic functions of Z with spatial period ℓ, while for $(\alpha = 6.5, \ell = 0.5)$, this is not the case. In the latter case, the condition for DL is not satisfied, $\phi_\pm(Z) \neq 0$ for $Z > 0$, hence, the light is not being localized. However, for the specific values of the normalized amplitude α=6.5 and the spatial period $\ell = 1.2477$, the condition for DL is satisfied, and light is confined in the initial injected guide at the propagation distances $Z_m = m\ell$; $m = 1, 2, \ldots$. For typical values [27] $C = 0.15\ \mathrm{mm}^{-1}$, λ=600 nm, $n_s = 1.5$ and $d = 15\ \mu\mathrm{m}$, this situation leads to L=8.32 mm and $A \simeq 14.5\ \mu\mathrm{m}$ for spatial period and amplitude of bent guides, respectively. In this case, the condition $L \gg A$ is satisfied.

To confirm the aforementioned results, Eq. (2) is solved numerically by Runge–Kutta–Fehlberg Method (an alternative approach is given in Eq. (10)). In our simulation, the evolution of real and imaginary parts of light amplitude are solved separately. Figs. 3 and 4 show the light intensity distribution for two different conditions, when light is injected into $n_0 = 50$ waveguide at the initial plane, i.e. $\Psi_n(Z = 0) = \delta_{n,n_0}$. In Fig. 3, the condition for DL is satisfied ($\alpha = 6.5$, $\ell = 1.2477$), and the light is localized dynamically, after every spatial period $\ell = 1.2477$ on the sinusoidal waveguides. Our investigation shows that this behavior is independent of the initial excited waveguide number n_0.

In contrast to Fig. 3, Fig. 4 shows the propagation pattern of light when DL is absent ($\alpha = 6.5$, $\ell = 0.5$). In this case, by increasing the normalized propagation distance Z, the width of initial profile increases and the light expands to the right guides endlessly.

Our study reveals that DL takes place under certain conditions, which depend on the amplitude and spatial period of the waveguides and the frequency of the incident light, i.e., at particular values of (α, ℓ). Whenever the condition is satisfied we get $\phi_\pm(Z) = \phi_\pm(Z + \ell)$ and $\phi_z(Z) = \phi_z(Z + \ell)$, which leads to DL. The (red) circles in Fig. 5 show several numerically obtained points (α, ℓ) in which DL is occurred. In addition, the (blue) solid line displays the fit to the numerical data points (with the least square error $R^2 = 0.999$), which is given by the following relation:

$$\ell_{DL}(\alpha) = \frac{4.11}{(\alpha - 2)^{0.85}}. \tag{11}$$

According to Fig. 5, for $\alpha \to 2$, the normalized spatial period of

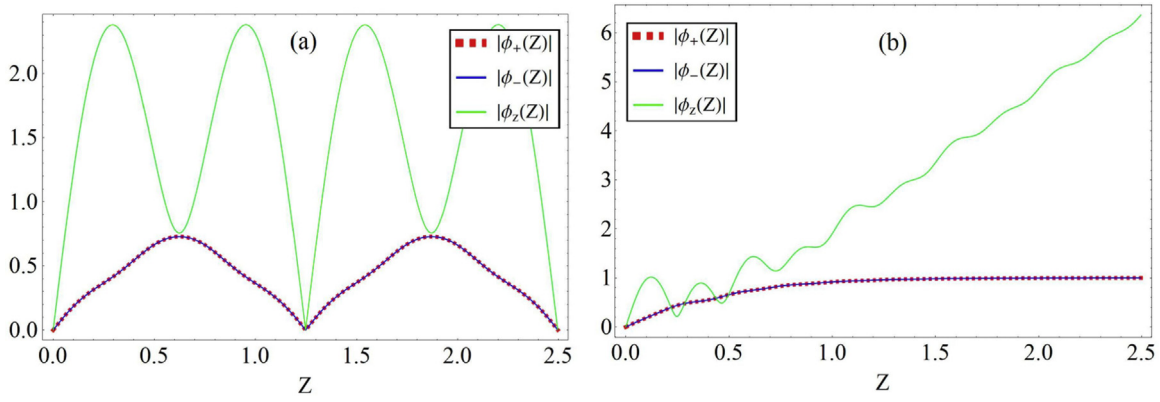

Fig. 2. Numerical solution of the system of equations (2) for (a) $\alpha = 6.5$, $\ell = 1.2477$ and (b) $\alpha = 6.5$, $\ell = 0.5$.

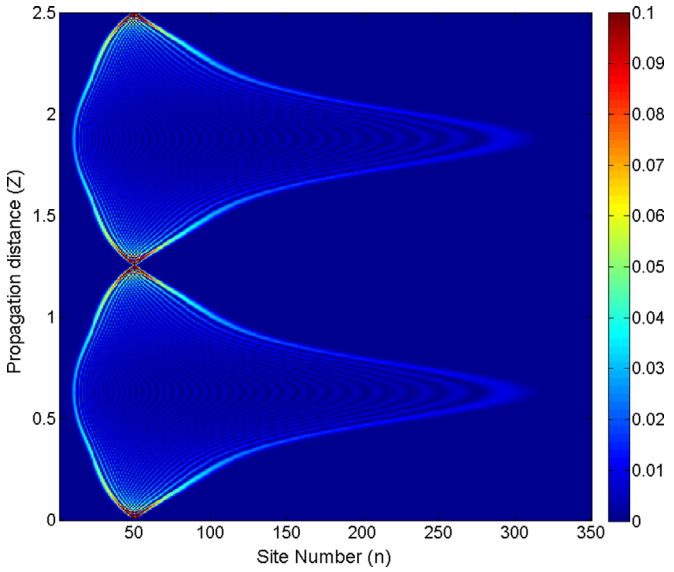

Fig. 3. Numerical results for light intensity distribution when DL takes place (α=6.5, ℓ = 1.2477) and light is injected into the waveguide labeled n_0 = 50 at the initial plane.

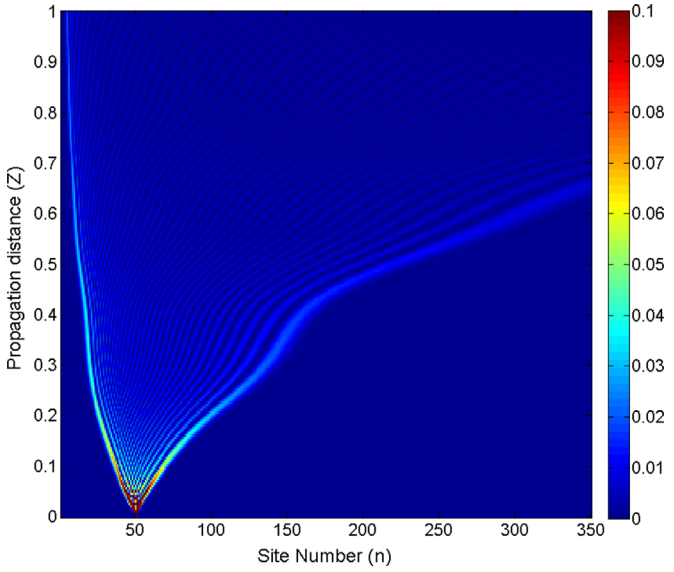

Fig. 4. Numerical results for light intensity distribution when DL is absent (α = 6.5, ℓ = 0.5) and light is injected into the waveguide n_0 = 50 at the initial plane.

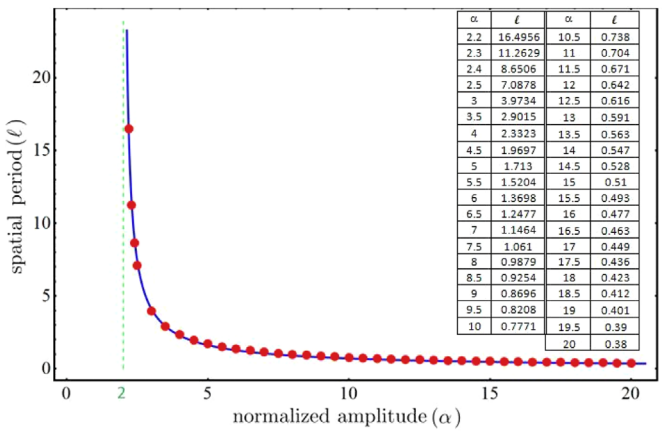

α	ℓ	α	ℓ
2.2	16.4956	10.5	0.738
2.3	11.2629	11	0.704
2.4	8.6506	11.5	0.671
2.5	7.0878	12	0.642
3	3.9734	12.5	0.616
3.5	2.9015	13	0.591
4	2.3323	13.5	0.563
4.5	1.9697	14	0.547
5	1.713	14.5	0.528
5.5	1.5204	15	0.51
6	1.3698	15.5	0.493
6.5	1.2477	16	0.477
7	1.1464	16.5	0.463
7.5	1.061	17	0.449
8	0.9879	17.5	0.436
8.5	0.9254	18	0.423
9	0.8696	18.5	0.412
9.5	0.8208	19	0.401
10	0.7771	19.5	0.39
		20	0.38

Fig. 5. Numerically obtained values (α, ℓ) in which DL takes place (red circles and inset table), and a fit through these data points (blue solid line). (For interpretation of the references to color in this figure caption, the reader is referred to the web version of this paper.)

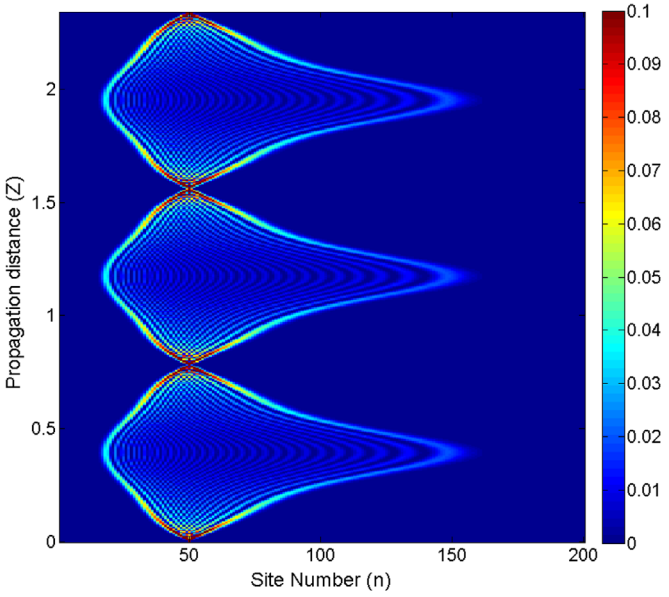

Fig. 6. Numerical results for light intensity distribution when DL occurs (α=10, ℓ = 0.7771) and light is injected into the waveguide n_0 = 50 at the initial plane.

waveguides must tend to infinity to get DL. Our study shows that DL is always absent whenever the normalized amplitude of sinusoidal waveguides (α) is lower than the critical value $\alpha_c = 2$. In other words, for $\alpha < \alpha_c$, the condition for DL is not satisfied for any finite value of ℓ. This can be understood in terms of our study on the spatial BO in squeezed photonic lattices [25]. The limit of $\ell \to \infty$ in Eq. (2), which happens for $\alpha \to 2$, renders straight optical waveguides (without curvature) that corresponds to the master equation of spatial BO in squeezed photonic lattices (Eq. (2) of Ref. [25]).

We have also found that the number of occupied waveguides is reduced by increasing the normalized amplitude α. Fig. 6 shows the dynamically localized intensity distribution of light for (α=10, ℓ = 0.7771) and n_0 = 50, which illustrates less occupied waveguides compared with Fig. 3 for α=6.5. Therefore, as the normalized amplitude of sinusoidal waveguides (α) is increased, the light expands over less numbers of waveguides within a period of DL. This sentence is plausible, because the DL is the result of bent waveguides. Moreover, the maximal pattern width takes place at the normalized propagation distances $Z = (2m + 1)\frac{\ell}{2}$.

This result can be confirmed by calculating the width of light intensity profile at the half period of bending guides versus the normalized amplitude α, which is defined as follow:

$$w^{(n_0)}(Z) = \left(\sum_{n=0}^{\infty} n^2 \left|\Psi_n^{(n_0)}(Z)\right|^2 - \left(\sum_{n=0}^{\infty} n \left|\Psi_n^{(n_0)}(Z)\right|^2 \right)^2 \right)^{1/2}. \quad (12)$$

Fig. 7 shows the maximal pattern width ($w^{(n_0)}(Z = \frac{l}{2})$) versus normalized amplitude α for two different initial excitation waveguide numbers. As can be seen in this figure, by increasing the normalized amplitude (α) of bending guides (corresponding to the decreasing of the period), the maximum width of the light intensity pattern decreases, which confirms the former results.

Due to the no-homogeneity of the coupling coefficients between neighbor waveguides as $C_n = C\sqrt{2n(2n-1)}$, the maximal pattern width also depends on to the initial excitation waveguide number (n_0). As shown in this figure, by increasing the initial

Please cite this article as: M.K. Nezhad, et al., Optics Communications (2016), http://dx.doi.org/10.1016/j.optcom.2016.01.082

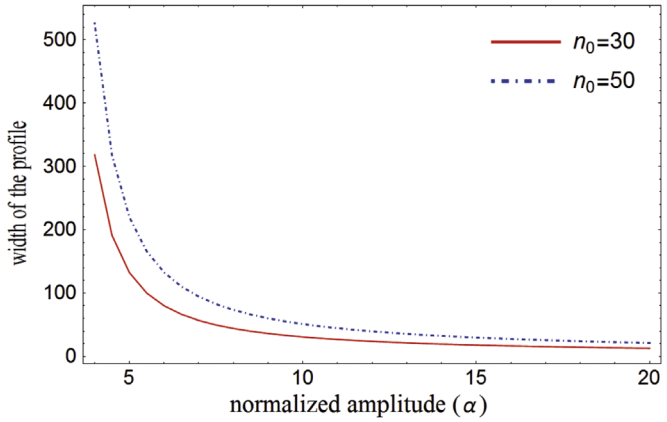

Fig. 7. The maximal pattern width versus normalized amplitude alpha for two initial excitation waveguide numbers $n_0 = 30$ and $n_0 = 50$.

excitation waveguide number, the maximal pattern width is also increased.

It is also interesting to investigate the evolution of a Gaussian beam along the waveguides, when the condition of DL is satisfied. To this end, a Gaussian beam of width σ and centered at n_0,

$$\Psi_n(Z=0) = \exp\left[-\frac{(n-n_0)^2}{4\sigma^2}\right], \tag{13}$$

is injected into the lattice at the initial plane. The intensity profile of the light for the Gaussian input beam with $\sigma = 10$ and $n_0 = 50$ is shown in Fig. 8. Comparing Fig. 8 with Fig. 6, (with the same $\alpha = 10$ and $\ell = 0.7771$), manifests that, in both cases, the intensity profile is repeated periodically after a propagation distance $\ell = 0.7771$, although their pattern are different. In the case of single site excitation, the variation in the width of the profile is stronger than its mean center, while for the Gaussian input profile, the converse is true.

As mentioned previously, for $\ell \to \infty$, Eq. (2) describes the light evolution in a straight squeezed-like waveguide array owning a linear transverse gradient 2α on the propagation constants. This is a structure in which the spatial BO can occur, and was investigated in our earlier work [25]. Hence, in order to complete our analysis, we compare the results of present study (DL) with BO in the

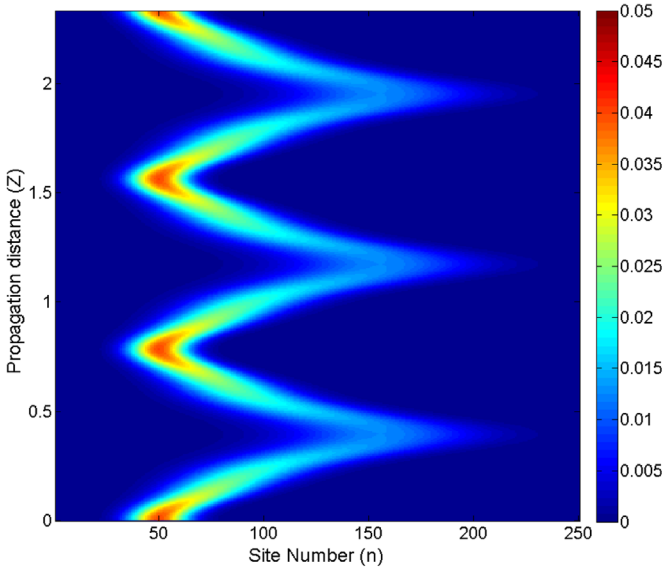

Fig. 8. Numerical results for light intensity distribution for which DL takes place ($\alpha = 10$ and $\ell = 0.7771$) and a Gaussian light beam centered on the $n_0 = 50$ and width $\sigma = 10$ is injected into the initial plane.

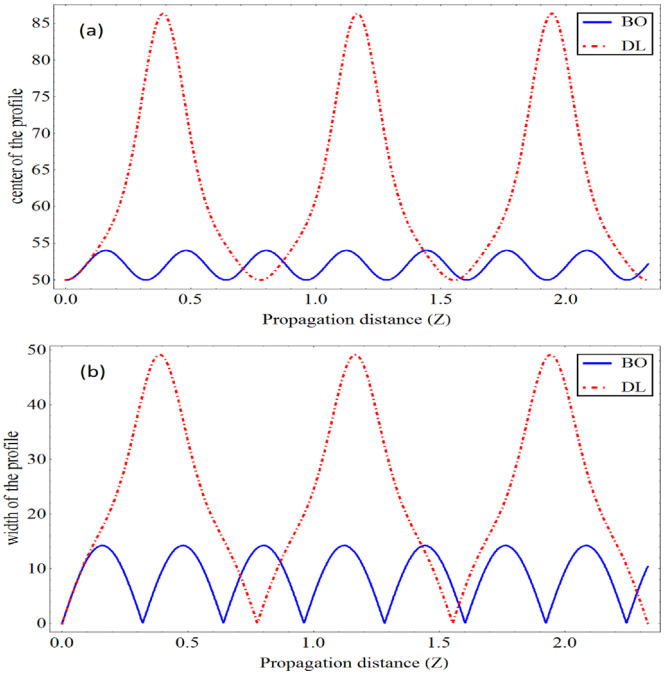

Fig. 9. Variation of (a) the center, and (b) the width of the light intensity profile for BO (with $\alpha = 10$) and DL (with $\alpha = 10$ and $\ell = 0.7771$) when light is injected into the waveguide labeled $n_0 = 50$ at the initial plane.

squeezed-like photonic lattices. BO and DL are two models of coherent quantum transport phenomena with the same features of periodic propagation pattern, while their origins are different. In both systems, there is a critical value $\alpha_c = 2$ at which the phase transition is occurred. In the straight squeezed-like lattices (with a linear transverse gradient on the propagation constants), BO appears for $\alpha > \alpha_c$, and the intensity profile is periodic with the spatial period $\ell_{BO}(\alpha) = \frac{\pi}{\sqrt{\alpha^2-4}}$ (see [25]). The comparison of ℓ_{DL} with ℓ_{BO} show that, for any $\alpha > \alpha_c$, the spatial period of DL is greater than the spatial period of BO, i.e. $\ell_{DL}(\alpha) > \ell_{BO}(\alpha)$. Moreover, we have realized that, for the same value of $\alpha > \alpha_c$, the variation in the width and the mean center of the BO profile is less than the corresponding values for DL. All of these results are summarized in Fig. 9, in which the center $C^{(n_0)}(Z) = \sum_{n=0}^{\infty} n|\Psi_n(Z)|^2$ and the width $w^{(n_0)}(Z)$ of BO and DL profiles (with the same $\alpha = 10$ and initial injected waveguide number $n_0 = 50$) are plotted versus the propagation distance Z.

At the end, we should emphasise that the DL in squeezed-like photonic lattice can be observed experimentally only with few waveguides. Fig. 10 shows the light intensity distribution for $\alpha = 16$ and $\ell = 0.477$ in the lattice with 12 guides. For previous typical values, this condition leads to $L = 3.18$ mm and $A = 5.22$ μm, which is accessible in experiment.

4. Conclusion

We have studied the DL of light in sinusoidal bent squeezed-like photonic lattices. Our investigation manifests that DL is emerged for the normalized amplitude $\alpha > 2$, at a specific value of the spatial period ℓ, which enhances by decreasing α (see Fig. 5). Thus, by increasing the amplitude, the spatial period of sinusoidal waveguides have to be decreased to observe DL. This dynamically localized behavior comes from the cancellation of diffraction after each spatial period ℓ. Another aspect of our study is that light expands over less numbers of guides as long as α is increased. In addition, the comparison between BO and DL in squeezed-like

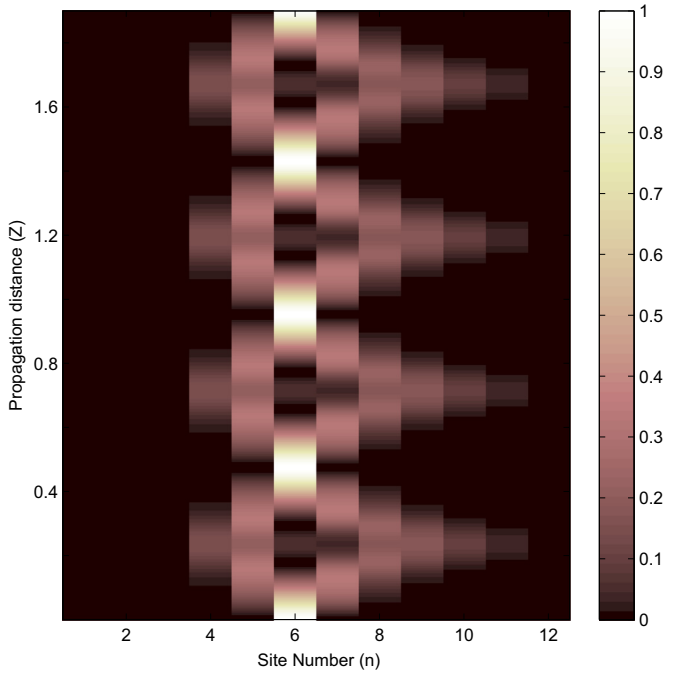

Fig. 10. Numerical results for light intensity distribution when DL occurs (α=16, ℓ = 0.477) and light is injected into the waveguide n_0 = 6 at the initial plane.

photonic lattices reveals that in both phenomena a phase transition occurs at the critical normalized amplitude $\alpha_c = 2$. Moreover, for the same value of $\alpha > \alpha_c$, the spatial period and the variation in the width and the mean center of the BO profile is less than the corresponding values for DL.

By carefully adjusting the spatial period and amplitude of guides, the DL in sinusoidal bent squeezed-like photonic lattice can be observed in experiment only with few guides.

DL takes place under certain condition on the sinusoidal bent squeezed-like photonic lattices, in spite of the fact that the semi infinite nature and inhomogeneity of coupling coefficients of these lattices are similar to the GF lattices. We hope that, the squeezed photonic lattices and the sinusoidal bent squeezed-like photonic lattices can be used to simulate classically another type of quantum and semi-classical Rabi oscillation (two-photon absorption), respectively.

References

[1] F. Bloch, Z. Phys. 52 (1928) 555.
[2] D.H. Dunlap, V.M. Kenkre, Phys. Rev. B 34 (1986) 3625.
[3] I.L. Garanovich, S. Longhi, A.A. Sukhorukov, Y.S. Kivshar, Phys. Rep. 518 (2012) 1.
[4] S. Longhi, Laser Photon Rev. 3 (2009) 3.
[5] F. Lederer, G.I. Stegeman, D.N. Christodoulides, G. Assanto, M. Segev, Y. Silberberg, Phys. Rep. 463 (2008) 1.
[6] G. Lenz, I. Talanina, C.M. de Sterke, Phys. Rev. Lett. 83 (1999) 963.
[7] T. Pertsch, P. Dannberg, W. Elflein, A. Brauer, F. Lederer, Phys. Rev. Lett. 83 (1999) 4752.
[8] R. Morandotti, U. Peschel, J.S. Aitchison, H.S. Eisenberg, Y. Silberberg, Phys. Rev. Lett. 83 (1999) 4756.
[9] H. Trompeter, W. Krolikowski, D.N. Neshev, A.S. Desyatnikov, A.A. Sukhorukov, Y.S. Kivshar, T. Pertsch, U. Peschel, F. Lederer, Phys. Rev. Lett. 96 (2006) 053903.
[10] M. Holthaus, Phys. Rev. Lett. 69 (1992) 351.
[11] S. Longhi, M. Marangoni, M. Lobino, R. Ramponi, P. Laporta, E. Cianci, V. Foglietti, Phys. Rev. Lett. 96 (2006) 243901.
[12] A. Szameit, I.L. Garanovich, M. Heinrich, A.A. Sukhorukov, F. Dreisow, T. Pertsch, S. Nolte, A. Tünnermann, S. Longhi, Y.S. Kivshar, Phys. Rev. Lett. 104 (2010) 223903.
[13] A. Szameit, I.L. Garanovich, M. Heinrich, A.A. Sukhorukov, F. Dreisow, T. Pertsch, S. Nolte, A. Tünnermann, Y.S. Kivshar, Nat. Phys. 5 (2009) 271.
[14] B.G. Klappauf, W.H. Oskay, D.A. Steck, M.G. Raizen, Phys. Rev. Lett. 81 (1998) 1203.
[15] D. Suqing, X.G. Zhao, Phys. Rev. B 61 (2000) 5442.
[16] M.M. Dignam, C.M. de Sterke, Phys. Rev. Lett. 88 (2002) 046806.
[17] O.V. Borovkova, V.E. Lobanov, Y.V. Kartashov, V.A. Vysloukh, L. Torner, Phys. Rev. A 91 (2015) 063825.
[18] I.G. Garanovich, A.A. Sukhorukov, Y.S. Kivshar, Phys. Rev. Lett. 100 (2008) 203904.
[19] A. Szameit, I.L. Garanovich, M. Heinrich, A.A. Sukhorukov, F. Dreisow, T. Pertsch, S. Nolte, A. Tunnermann, Y.S. Kivshar, Phys. Rev. Lett. 101 (2008) 203902.
[20] A. Perez-Leija, H. Moya-Cessa, A. Szameit, D.N. Christodoulides, Opt. Lett. 35 (2010) 14.
[21] R. Keil, A. Perez-Leija, F. Dreisow, M. Heinrich, H. Moya-Cessa, S. Nolte, D. N. Christodoulides, A. Szameit, Phys. Rev. Lett. 107 (2011) 103601.
[22] R. Keil, A. Perez-Leija, P. Aleahmad, H. Moya-Cessa, S. Nolte, D. N. Christodoulides, A. Szameit, Opt. Lett. 37 (2012) 18.
[23] A. Perez-Leija, R. Keil, A. Szameit, A.F. Abouraddy, H. Moya-Cessa, D. N. Christodoulides, Phys. Rev. A 85 (2012) 013848.
[24] S. Longhi, A. Szameit, J. Phys.: Condens. 25 (2013) 035603.
[25] M. Khazaei Nezhad, A.R. Bahrampour, M. Golshani, S.M. Mahdavi, A. Langari, Phys. Rev. A 88 (2013) 023801.
[26] S. Longhi, Phys. Rev. B 80 (2009) 033106.
[27] F. Dreisow, M. Heinrich, A. Szameit, S. Doring, S. Nolte, A. Tunnermann, S. Fahr, F. Lederer, Opt. Exp. 16 (2008) 3474.
[28] M.J. Ablowitz, Z.H. Musslimani, Physica D 184 (2003) 276.
[29] A. Szameit, F. Dreisow, T. Pertsch, S. Nolte, A. Tünnermann, Opt. Exp. 15 (2007) 1579.
[30] R.R. Puri, Mathematical Methods of Quantum Optics, Springer, Berlin, 2001.

Please cite this article as: M.K. Nezhad, et al., Optics Communications (2016), http://dx.doi.org/10.1016/j.optcom.2016.01.082